

Best Arm Identification Based Beam Acquisition in Stationary and Abruptly Changing Environments

Gourab Ghatak, *Member, IEEE*

Abstract—We study the initial beam acquisition problem in millimeter wave (mm-wave) networks from the perspective of best arm identification in multi-armed bandits (MABs). For the stationary environment, we propose a novel algorithm called concurrent beam exploration, CBE, in which multiple beams are grouped based on the beam indices and are simultaneously activated to detect the presence of the user. The best beam is then identified using a Hamming decoding strategy. For the case of orthogonal and highly directional thin beams, we characterize the performance of CBE in terms of the probability of missed detection and false alarm in a beam group (BG). Leveraging this, we derive the probability of beam selection error and prove that CBE outperforms the state-of-the-art strategies in this metric.

Then, for the abruptly changing environments, e.g., in the case of moving blockages, we characterize the performance of the classical sequential halving (SH) algorithm. In particular, we derive the conditions on the distribution of the change for which the beam selection error is exponentially bounded. In case the change is restricted to a subset of the beams, we devise a strategy called K-sequential halving and exhaustive search, K-SHES, that leads to an improved bound for the beam selection error as compared to SH. This policy is particularly useful when a near-optimal beam becomes optimal during the beam-selection procedure due to abruptly changing channel conditions. Finally, we demonstrate the efficacy of the proposed scheme by employing it in a tandem beam refinement and data transmission scheme.

I. INTRODUCTION

A. Context and Background

The millimeter wave (mm-wave) spectrum offers large bandwidths, enabling high data rates for future wireless applications [1]. However, it is highly susceptible to path loss and blockage due to the shorter wavelength [2]. To overcome such detrimental issues, the mm-wave transceivers employ beamforming using large antenna arrays [3]. Consequently, in mm-wave communication systems, initial beam selection plays a crucial role in establishing a reliable and high-quality link between the base station (BS) and the user equipment (UE) [4] [5]. In the case of beam-selection error or beam misalignment, the received signal quality at the UE deteriorates significantly thereby rendering communication infeasible [6].

The number of beams per synchronization signal block (SSB) can vary depending on the specific deployment and configuration of the network [7]. The exact number of beams per SSB is determined by the network operator and can be adjusted based on factors such as coverage requirements, network capacity, and radio resource management strategies. 3GPP specifies that multiple beams can be formed and transmitted by the base station (gNB) to cover different areas or sectors [8], which we also assume in the first part of our work. The number

of beams can be dynamically configured and can vary from one gNB to another.

To perform initial beam acquisition in mm-wave systems, researchers have investigated several technologies such as beam sweeping [9], channel estimation [6], compressed sensing [10], hybrid beamforming [11], and machine-learning [12], [13]. Beam sweeping involves transmitting signals using different beamforming directions over a predefined set of beams. The receiver then measures the received signal quality for each beam and reports it back to the transmitter. Based on this feedback, the transmitter selects the beam with the highest received signal strength or quality. An exhaustive search of the beam space is associated with high overheads and leads to high initial access delays. To overcome this, researchers have proposed compressed sensing methods, where the BS sends a compressed version of the beam codebook to the UE [10]. Hybrid beamforming is often employed to strike a balance between performance and complexity [11]. In this approach, initially, analog beamforming is performed at the transmitter using a limited number of radio frequency (RF) chains, which reduces the complexity. The receiver measures the signal quality for each analog beam, and the selected beam index is fed back to the transmitter. Then, digital beamforming is applied on the selected beam at the transmitter to further refine the beamforming gain.

On the contrary, several approaches for initial access involve the estimation of the channel characteristics between the transmitter and receiver [14], [15]. By exploiting the estimated channel information, such as arrival and departure angles, the transmitter can make informed decisions regarding initial beam selection. This falls under the larger umbrella of localization-assisted initial access [6]. Recently, machine learning algorithms have been utilized to learn and predict the optimal beam selection based on various channel and environment parameters [16]. In particular, by training models with large datasets, the transmitter can predict the best beamforming parameters for a given set of conditions, reducing the need for exhaustive beam search procedures [17].

The specific method chosen for initial beam selection depends on the system requirements, available resources, and implementation constraints. Beam training and selection are iterative processes, and continuous adaptation may be necessary to maintain an optimal link in dynamic mm-wave environments. However, the issue of a changing environment during the beam selection procedure is largely unaddressed.

B. Related Work

Authors in [18] proposed antenna architectures that generate a collection of well-defined, high-gain, orthogonal beams. Due to the orthogonal nature of each beam and their minimal

The author is with the Department of Electrical Engineering at the Indian Institute of Technology (IIT) Delhi, New Delhi, India 110016. Email: gghatak@ee.iitd.ac.in.

coupling with other beams, these transmit beams possess inherent independence and exhibit relatively low correlation. In our work, we consider a similar beamforming scheme characterized by thin, highly directional beams which are independent of each other.

Alkhateeb *et al.* [19] designed an initial beam association method based on beam sweeping and downlink control pilot reuse. Typically, hierarchical and multi-resolution codebooks result in reduced initial access delay. In this regard, Wang *et al.* [9] devised an efficient multi-resolution beam search technique that initiates with wide beams and progressively narrows them down until identifying the optimal beam. Nevertheless, the beam resolution requires adjustment at each stage. Wu *et al.* [20] presented a technique for rapid and precise beam alignment in multi-path channels within a point-to-point mm-wave system. The method capitalizes on the correlation structure among beams, extracting information from neighboring beams to identify the optimal beam efficiently, rather than searching through the entire beam space.

There exists extensive research literature on beam selection strategies for 5G and beyond systems, an exhaustive discussion of which is out of scope of the current discussion. Instead, we enlist below the multi-armed bandit (MAB) based approaches for the beam selection problem and refer the reader to the work by Giordani [4] and the references therein for a thorough discussion on the other techniques.

Recently, MAB frameworks have been employed to study the problem of efficient initial access. It is interesting to note that the two settings of the best arm identification problem in MABs - the fixed budget setting and the fixed confidence setting correspond to two beam acquisition requirements - fixed beam selection deadline, and fixed beam selection error. Hashemi *et al.* [21] have studied contextual bandits for beam alignment. Specifically, they address an online stochastic optimization scenario where the objective is to maximize the directivity gain of the beam alignment policy over a specific time frame. By leveraging the inherent correlation and unimodality properties of the model, the authors illustrate that the inclusion of contextual information enhances performance. The work by Va *et al.* [22] utilized a UCB-based framework to create an online learning algorithm for selecting and refining beam pairs. The algorithm initially learns coarse beam directions from a predefined beam codebook and subsequently refines the identified directions to align with the power angular spectrum's peak at that specific position. Hussain *et al.* [23] developed an innovative scheme for beam pair alignment utilizing Bayesian MABs. The primary objective of this scheme was to maximize both the alignment probability and the throughput of data communication. More recently, Wei *et al.* developed a bandit-based initial beam selection algorithm named two-phase heteroscedastic track-and-stop (2PHT&S) [24]. The authors formulated the beam selection as a fixed-confidence pure exploration problem. The authors assumed a correlation structure among beams, considering that the information from nearby beams is similar. Additionally, the algorithm takes exploits the heteroscedastic property that the variance of the reward of an arm is related to its mean. 2PHT&S groups all beams into several beam sets such that the optimal beam set is first

selected and the optimal beam is identified in this set.

C. Motivation

In almost all of the research above, the authors did not provide any insight into the performance of their algorithms in a non-stationary environment. Our formulation also considers the heteroscedastic Gaussian distribution and for the stationary environment, we demonstrate that for highly directional thin beams, CBE outperforms 2PHT&S. Additionally, we investigate an algorithm tuned to a changing environment.

D. Contributions and Organization

The main contributions in this work are as follows.

- For the stationary environment we propose and characterize a novel initial beam acquisition algorithm, concurrent beam-exploration (CBE). The main innovation in CBE is the formation of beam groups (BGs) based on the beam indices, followed by concurrent multi-beam detection to identify the BGs in which the UE is present. Then, the index of the best beam is decoded for service.
- We prove that in the case of highly directional beams that are characterized by negligible side-lobe gains, the detection statistic reduces to a generalized Chi-square distributed random variable. We derive the probability of missed detection and the probability of false alarms for the BGs. Leveraging this, we prove that CBE reduces the probability of beam selection error as compared to the state-of-the-art hierarchical beam selection procedures.
- For the case of intermittent blockages, i.e., when a previously sub-optimal beam becomes optimal during the beam selection procedure, the performance of CBE deteriorates significantly. For this piece-wise stationary environment, we characterize the performance of the sequential halving (SH) algorithm, which is popular for best arm identification in bandit environments. To the best of our knowledge, ours is the first work that rigorously characterizes the performance of SH in an abruptly-changing environment. We show that the upper bound of SH consists of an exponential term and a term dependent on the distribution of the location of the change. Accordingly, we derive conditions on the distribution of the change in order to guarantee an exponential bound for SH in the presence of a single change.
- For the case when the change occurs in one of the best K arms, we propose a novel algorithm called K -sequential halving followed by exhaustive search (K -SHES) and demonstrate that it outperforms not only SH but also other state-of-the-art algorithms for initial beam acquisition. To the best of our knowledge, this is the first attempt at algorithm design for beam acquisition in a changing environment. We also highlight its limitations, specifically for the cases of early change.
- Finally, as a case study to test the efficacy of K -SHES, we employ it in a tandem beam refinement and data communication system. Based on that, we derive the system design rules for selecting an optimal beam dictionary size

and the optimal fractional resources allotted to the beam refinement phase of the system.

The rest of the paper is organized as follows. We introduce the system model and define the problem statement for both the stationary and the non-stationary case in Section II. We focus on the stationary environment in Section III and propose and characterize the CBE algorithm. The abruptly changing environment is considered in Section IV. The heuristic hybrid policy K-SHES is proposed in Section V. Some numerical results and the case study are discussed in Section VI. Finally, the paper concludes in Section VII.

II. SYSTEM MODEL AND PROBLEM STATEMENT

We consider the propagation environment with limited scattering (typical for mm-wave channels) and adopt the commonly-used geometric channel model [24]. Let us consider a uniform linear array (ULA), however, it will shortly be apparent that the framework can be applied to a uniform planar array (UPA) since the analysis follows only from the beam directions. The beamforming codebook \mathcal{N} of size N is

$$\mathcal{C} \triangleq \{\mathbf{f}_i = \mathbf{a}(-1 + 2i/K) \mid i = 0, 1, \dots, N-1\}, \quad (1)$$

where $\mathbf{a}(\cdot)$ denotes the array response vector. The structure of $\mathbf{a}(\cdot)$ for ULA can be found in [24] and is skipped here for brevity. The received signal in case only \mathbf{f}_i is activated is

$$y_i = \sqrt{P}\mathbf{h}_i^H \mathbf{f}_i + n,$$

where \mathbf{h} is the channel vector. Thus, the received power is

$$R_i = P|\mathbf{h}_i^H \mathbf{f}_i|^2 + |n|^2 + 2\sqrt{P}\mathbb{R}(\mathbf{h}_i^H \mathbf{f}_i n^*),$$

where $\mathbb{R}(\cdot)$ denotes the real part of the argument. Since the noise power is negligible, the received power is Gaussian distributed with mean $\mu_i = P|\mathbf{h}_i^H \mathbf{f}_i|^2$ and variance $\sigma_i^2 = 2P|\mathbf{h}_i^H \mathbf{f}_i|^2\sigma^2 = 2\sigma^2\mu_i$ [24]. In what follows, we formulate two problem statements P_1 and P_2 , for the stationary and the abruptly-changing case respectively. In addition, for the stationary environment, we make an additional assumption that the best beam, i.e., the beam in which the user is aligned has a gain G , while all the other beams, i.e., the ones not aligned towards the user have a gain g . Note that this assumption is only for the stationary environment, while for the abruptly changing environment, the model is more general as described later.

A. Stationary Environment Problem

The problem of the best beam identification is the same as selecting the beam with the highest μ_i within a beam selection deadline T .

$$\begin{aligned} P_1 : \quad & \text{Find } \arg \max_i \mu_i, \\ \text{st} \quad & R(t) \sim \mathcal{N}(\mu_i, \sigma_i), \quad \forall i, \forall t \in [T] \\ \text{within} \quad & T. \end{aligned}$$

The critical challenge is the fact that the beam with the highest μ_i is also the same with the highest σ_i and accordingly, a higher number of samples is needed to estimate μ_i . At the

end of T , let the selected beam by an algorithm/policy \mathcal{Z} be $f_{\mathcal{Z}}$. Then the probability of beam selection error is given as

$$\mathcal{P}_e^{\mathcal{Z}} = \mathbb{P}(f_{\mathcal{Z}} \neq \max\{\mathbf{f}_i\}),$$

where the subscript $e \in \{\text{NC}, \text{C}\}$ stands for either a stationary (NC: no-change) or non-stationary (C : changing) environment. The typical benchmark used for comparing proposed beam selection algorithms is the exhaustive search [25], where each beam is activated sequentially and based on multiple measurements for each beam, the best beam is selected. Other popular algorithms with which we compare our results are hierarchical search [26] for the stationary and non-stationary case and a variant of track and stop [24] for the non-stationary case. First, let us note that the beam selection error for the exhaustive search approach is obvious from the Chernoff bound [27] as follows.

Lemma 1. *For single beam activation, with $T_i \in \mathbb{N}$ observations, the estimate $\hat{\mu}_i$ of μ_i is close to μ_i is given by*

$$\mathbb{P}(|\hat{\mu}_i - \mu_i| \geq \epsilon) \leq \exp\left(-\frac{T_i \epsilon^2}{4\sigma_i^2 \mu_i}\right).$$

In the case of fixed-budget exploration, equal temporal resources are allotted to each beam, i.e., $T_i = \frac{T}{N}$. Thus, in case of an exhaustive search in a stationary environment, the probability of beam-selection error is upper bounded by

$$\begin{aligned} \mathcal{P}_{\text{NC}}^{\text{ES}}(T) &\leq \sum_{i \neq 1} \mathbb{P}(|\hat{\mu}_i - \mu_1| \geq \epsilon) \\ &\leq N \exp\left(-\frac{T \Delta_{\min}^2}{8N \sigma^2 \mu_{\max}}\right). \end{aligned} \quad (2)$$

In the first part of the paper, i.e., in Section III, we propose a grouped exploration strategy that outperforms not only this benchmark but also the popular hierarchical search algorithm for highly directional beams.

B. Abruptly Changing Environment Problem

In the second part of this paper, i.e., in Section IV we consider the scenario in which the environment changes abruptly. At a time slot t within the beam-selection deadline T , the mean of a sub-optimal beam \mathbf{f}_j changes from μ_j^- to μ_j^+ so that it becomes optimal for all time slots beyond t . This is typical in cases where the optimal beam is blocked during the initial parts of the beam selection process and the blockage shifts during the beam selection process. The challenge here is to still identify the best beam at the beam selection deadline T as described below.

$$\begin{aligned} P_2 : \quad & \arg \max_i \mu_i(T), \\ \text{st} \quad & R(t) \sim \mathcal{N}(\mu_i(t), \sigma_i(t)), \quad \forall i, \forall t \in [T] \\ & \mu_i(t) = \mu_i, \quad \forall i \neq j, \forall t, \\ & \mu_j(t) = \mu_j^-, \quad 0 \leq t \leq t_c, \\ & \mu_j(t) = \mu_j^+, \quad t_c < t \leq T, \\ \text{within} \quad & T. \end{aligned}$$

Note that the parameters for all other beams except \mathbf{f}_j remain constant.

Symbol	Definition
\mathcal{N}, N	Set of beams, number of beams.
\mathbf{f}_i	i -th beam.
T	Beam selection deadline.
$\mu_i(t)$	Mean of the i -th beam at time t .
μ_j^-	Mean of the j -th beam before change.
μ_j^+	Mean of the j -th beam after change.
Δ_c	Change in the means, $\Delta_c = \mu_j^+ - \mu_j^-$.
$\Delta_{i,j}^+$	$\mu_i - \mu_j^+$.
$\Delta_{i,j}^-$	$\mu_i - \mu_j^-$.
g, G	Gain of the incorrect and best beams, respectively in the stationary case.
B_k	k -th BG.
\mathbf{R}_{B_k}	Observations/Rewards from the k -th BG in CBE.
μ_1, σ_1^2	The mean and the variance of \mathbf{R}_{B_k} given the user is present in the k -th BG for CBE.
μ_0, σ_0^2	The mean and the variance of \mathbf{R}_{B_k} given the user is not present in the k -th BG for CBE.
K	Maximum index of beam which undergoes a change.
t_c	Time slot of change.
n_{r_c}	Change round in the SH algorithm.
n'	Change slot conditioned on the change round.
$F_{n'}(n n_{r_c})$	conditional CDF of n' given r_c .
Δ_{\min}	Minimum difference between the means of beams. $\Delta_{\min} = 0$ for CBE.
μ_{\max}	Maximum mean of a beam.
σ_{\max}^2	$2\sigma^2\mu_{\max}$.

Table I: List of notations

III. INDEXED EXPLORATION FOR STATIONARY ENVIRONMENT

Let us first analyze the stationary environment. The first step for CBE is to form BGs as discussed below.

A. Beam Grouping

The i -th beam \mathbf{f}_i is added to the BG B_k , $k = 1, 2, \dots, d$ if and only if the binary representation of i has a "1" in the k -th binary place. In other words, \mathbf{f}_i is added to B_k if $\text{bin2dec}(\text{dec2bin}(i) \text{ AND } \text{onehot}(k)) \neq 0$, where $\text{bin2dec}()$ and $\text{dec2bin}()$ are respectively operators that convert binary numbers to decimals and decimal numbers to binary. Additionally, $\text{onehot}(k)$ is a binary number with all zeros except 1 at the k -th binary position. AND is the bit-wise AND operator. This strategy for creating super-arms is inspired by the classical forward error correcting strategy due to Hamming, which enables detection and correction of single-bit errors [28]. Such a grouping strategy was explored in [29] for fast detection of changes in a classical bandit environment. However, here we leverage the same for quick identification of the best beam.

Example: Let us elaborate this further with an illustrative example by considering $N = 16$. Fig. 1 shows the following grouping for the beams - i) B_1 - Beams with '1' in the first binary place - $\mathbf{f}_1, \mathbf{f}_3, \mathbf{f}_5, \mathbf{f}_7, \mathbf{f}_9, \mathbf{f}_{11}, \mathbf{f}_{13}$, and \mathbf{f}_{15} , ii) B_2 - Beams with '1' in the second binary place - $\mathbf{f}_2, \mathbf{f}_3, \mathbf{f}_6, \mathbf{f}_7, \mathbf{f}_{10}, \mathbf{f}_{11}, \mathbf{f}_{14}$, and \mathbf{f}_{15} , iii) B_3 - Beams with '1' in the third binary place - $\mathbf{f}_4, \mathbf{f}_5, \mathbf{f}_6, \mathbf{f}_7, \mathbf{f}_{12}, \mathbf{f}_{13}, \mathbf{f}_{14}$, and \mathbf{f}_{15} , and iv) B_4 - Beams with '1' in the fourth binary place - $\mathbf{f}_8, \mathbf{f}_9, \mathbf{f}_{10}, \mathbf{f}_{11}, \mathbf{f}_{12}, \mathbf{f}_{13}, \mathbf{f}_{14}$, and \mathbf{f}_{15} .

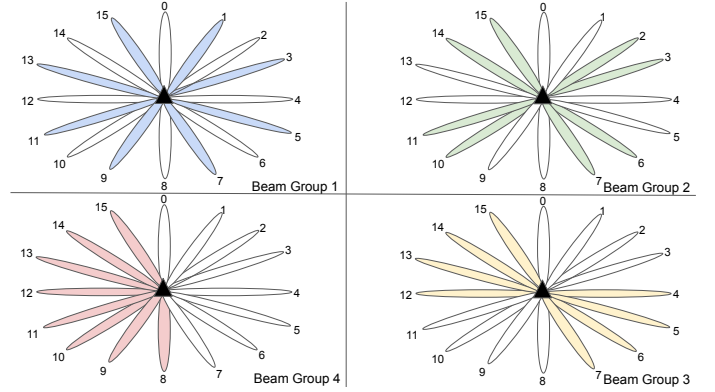


Fig. 1. Illustration of BG

B. Rewards

In case the BG B_k is employed to measure the downlink power, the received power is given as

$$P_{B_k} = \sum_{\mathbf{f}_i \in B_k} \frac{2P_t}{N} |\mathbf{h}^H \mathbf{f}_i|^2 + |n|^2 + \mathbb{R} \left(2 \sum_{\mathbf{f}_i \in B_k} \sqrt{\frac{P_t}{N}} \mathbf{h}^H \mathbf{f}_i n^1 + 2 \sum_{\mathbf{f}_i \in B_k} \sum_{\mathbf{f}_j \in B_k, \mathbf{f}_j \neq \mathbf{f}_i} \frac{P_t}{N} \mathbf{f}_i^H \mathbf{h} \mathbf{h}^H \mathbf{f}_j \right),$$

Similar to [24], we assume that the noise variance is much smaller than the transmit power. Additionally, since we assume highly directional beams [18], we neglect the contribution of $\mathbf{f}_i^H \mathbf{h} \mathbf{h}^H \mathbf{f}_j$ as either $\mathbf{f}_i^H \mathbf{h}$ or $\mathbf{f}_j^H \mathbf{h}$ is low for $i \neq j$. Accordingly, the variable P_{B_k} is approximately a Gaussian random variable with mean $\mu_{B_k} = \sum_{\mathbf{f}_i \in B_k} \frac{P_t}{N} |\mathbf{h}^H \mathbf{f}_i|^2 = \sum_{\mathbf{f}_i \in B_k} \frac{2\mu_i P_t}{N}$ and variance $\sigma_{B_k}^2 = 2 \sum_{\mathbf{f}_i \in B_k} \frac{P_t}{N} |\mathbf{h}^H \mathbf{f}_i|^2 \sigma^2 = \sum_{\mathbf{f}_i \in B_k} \frac{2\mu_i P_t \sigma^2}{N}$.

C. Beam Selection Strategy

The beam selection strategy for CBE is summarized in Algorithm 1. We divide the total initial access time into $\log N$ rounds and allot each round to one BG¹. Then, all the beams of a BG are activated to detect the presence of the user in that particular BG. Assume that $\mathbb{1}(B_k)$ indicates the presence of the user in BG B_k . Then, the user detection is based on the classical likelihood ratio test. Note that the conditional probability density functions (PDFs) of \mathbf{R}_{B_k} given that the user is respectively present and absent in the BG B_k , are

$$f_{\mathbf{R}_{B_k}|\mathbb{1}(B_k)}(\mathbf{y} | 1) = \prod_{j=1}^{T_{B_k}} \frac{1}{\sigma_1^2 \sqrt{2\pi}} \exp \left[-\frac{(y_j - \mu_1)^2}{2\sigma_1^2} \right],$$

$$f_{\mathbf{R}_{B_k}|\mathbb{1}(B_k)}(\mathbf{y} | 0) = \prod_{j=1}^{T_{B_k}} \frac{1}{\sigma_0^2 \sqrt{2\pi}} \exp \left[-\frac{(y_j - \mu_0)^2}{2\sigma_0^2} \right].$$

Here,

$$\mu_0 = g, \quad (3a)$$

$$\mu_1 = \frac{2}{N} \left(\left(\frac{N}{2} - 1 \right) g + G \right), \quad (3b)$$

$$\sigma_0^2 = 2g\sigma^2, \quad (3c)$$

$$\sigma_1^2 = \frac{4\sigma^2}{N} \left(\left(\frac{N}{2} - 1 \right) g + G \right). \quad (3d)$$

Accordingly, the log-likelihood ratio (LLR) is evaluated as

$$\begin{aligned} \text{LLR}(\mathbf{R}_{B_k}) &= \frac{\sigma_0}{\sigma_1} + \left[\sum_{j=1}^{T_{B_k}} -\frac{(y_j - \mu_1)^2}{2\sigma_1^2} + \frac{(y_j - \mu_0)^2}{2\sigma_0^2} \right] \\ &= \frac{\sigma_0}{\sigma_1} + \left[\sum_{j=1}^{T_{B_k}} \frac{1}{\sigma_0^2 \sigma_1^2} (y_j^2 (\sigma_1^2 - \sigma_0^2) + \right. \\ &\quad \left. 2y_j (\mu_1 \sigma_0^2 - \mu_0 \sigma_1^2) + (\sigma_1^2 \mu_0^2 - \mu_1^2 \sigma_0^2)) \right], \end{aligned}$$

where, interestingly, substituting (3), we get $\mu_1 \sigma_0^2 - \mu_0 \sigma_1^2 = 0$. Thus,

$$\begin{aligned} \text{LLR}(\mathbf{R}_{B_k}) &= \frac{\sigma_0}{\sigma_1} + T_{B_k} \left(\frac{\mu_0^2}{\sigma_0^2} - \frac{\mu_1^2}{\sigma_1^2} \right) + \sum_{j=1}^{T_{B_k}} y_j^2 \frac{\sigma_1^2 - \sigma_0^2}{\sigma_1^2 \sigma_0^2} \\ &= \sqrt{\frac{Ng}{2g'}} - T_{B_k} \frac{G - g}{N\sigma^2} + \frac{2}{N} \frac{g' - g}{\sigma^2 g'} \sum_{j=1}^{T_{B_k}} y_j^2, \end{aligned}$$

where

$$g' = \left(\frac{N}{2} - 1 \right) g + G.$$

Conveniently, our test statistic and the decision rule for BG B_k is

$$\|\mathbf{R}_{B_k}\|^2 = \sum_{j=1}^{T_{B_k}} y_j^2 \underset{\text{user not detected}}{\overset{\text{user detected}}{\geq}} \gamma, \quad (4)$$

where

$$\gamma = \frac{4gg'\sigma^2}{\frac{2}{N}g' - g} \left[1 - \sqrt{\frac{Ng}{2g'}} - T_{B_k} \left(\frac{g - G}{N\sigma^2} \right) \right].$$

Finally, based on the detection of the user in different BGs, the best beam is identified as the one that belongs to all the BGs in which the user is detected. For this let us define a new sequence of sets as

$$C_k = \begin{cases} B_k; & \text{If the user is detected in } B_k, \\ B_k^C; & \text{If the user is not detected in } B_k. \end{cases} \quad (5)$$

Then, the optimal beam is identified as \mathbf{f}_j , where $\mathbf{f}_j = \bigcap_{k=1}^{\log N} C_k$. In case the user is not detected in any of the BGs, the optimal beam is identified as \mathbf{f}_0 .

User in	Detected	Not detected
\mathbf{f}_0	-	B_1, B_2, B_3 and B_4
\mathbf{f}_1	B_1	B_2, B_3 , and B_4
\mathbf{f}_2	B_2	B_1, B_3 , and B_4
\mathbf{f}_3	B_1 and B_2	B_3 and B_4
\mathbf{f}_4	B_3	B_1, B_2 , and B_4
\mathbf{f}_5	B_1 and B_3	B_2 and B_4
\mathbf{f}_6	B_2 and B_3	B_1 and B_4
\mathbf{f}_7	B_1, B_2 , and B_3	B_4
\mathbf{f}_8	B_4	B_1, B_2 , and B_3
\mathbf{f}_9	B_1 and B_4	B_2 and B_3
\mathbf{f}_{10}	B_2 and B_4	B_1 and B_3
\mathbf{f}_{11}	B_1, B_2 , and B_4	B_3
\mathbf{f}_{12}	B_3 and B_4	B_1 and B_2
\mathbf{f}_{13}	B_1, B_3 , and B_4	B_2
\mathbf{f}_{14}	B_2, B_3 , and B_4	B_1
\mathbf{f}_{15}	B_1, B_2, B_3 and B_4	-

Table II: Exhaustive list of the combination of the BGs in which the user is detected.

Let us recall the illustration in Fig. 1. Corresponding to this case of 16 beams and 4 BGs, Table II exhaustively enlists the cases of beam identification. As an example, if the user is detected in B_1 but not in any other BG, then the beam \mathbf{f}_0 is selected for it. Similarly, if the user is detected in all the BGs, then the beam \mathbf{f}_{15} is identified as the best beam.

Algorithm 1 CBE

- 1: **Input:** $[\mathbf{F}]$
 - 2: Create BGs ($[\mathbf{F}]$)
 - 3: **for** $k = 1$ to $\log N$ **do**
 - 4: - Transmit using B_k for T_{B_k} slots and observe \mathbf{R}_{B_k} .
 - 5: - Detect whether the user is present in BG B_k using (4).
 - 6: - Create sequence of sets C_k using (5).
 - 7: **end for**
 - 8: **Return:** Optimal beam \mathbf{f}_j , where $\mathbf{f}_j = \bigcap_{k=1}^{\log N} C_k$.
-

¹ All logarithms in this paper unless otherwise stated have a base 2.

D. Characterization of the Test Statistic

We note that for the BG B_k , $\frac{\|\mathbf{R}_{B_k}\|^2}{\sigma_l^2}$ has a non-central Chi-squared distribution with T_{B_k} degrees of freedom and a non-centrality parameter $T_{B_k} \frac{\mu_l}{\sigma_l^2}$, where $l \in \{0, 1\}$, respectively denoting the presence and the absence of the user in the BG B_k . Mathematically, if $y_i \sim \mathcal{N}(\mu_l, \sigma_l^2)$, we have

$$\frac{\|\mathbf{R}_{B_k}\|^2}{\sigma_l^2} \sim \chi_{\text{NC}}^2 \left(T_{B_k}, T_{B_k} \frac{\mu_l^2}{\sigma_l^2} \right), \quad (6)$$

where $\chi_{\text{NC}}^2(a, b)$ is the non-central Chi-squared distribution with a degrees of freedom and non-centrality parameter b . Accordingly, the conditional cumulative density function (CDF) of $\frac{\|\mathbf{R}_{B_k}\|^2}{\sigma_l^2}$ is

$$\begin{aligned} F_{\frac{\|\mathbf{R}_{B_k}\|^2}{\sigma_l^2} | \mathbb{1}(B_k)=l}(x) &= \mathbb{P} \left(\frac{\|\mathbf{R}_{B_k}\|^2}{\sigma_l^2} \leq x \mid \mathbb{1}(B_k) = l \right) \\ &= 1 - \mathcal{Q}_{\frac{T_{B_k}}{2}} \left(\sqrt{T_{B_k}} \frac{\mu_l}{\sigma_l}, \sqrt{x} \right), \end{aligned} \quad (7)$$

where

$$\begin{aligned} \mathcal{Q}_{\frac{T_{B_k}}{2}} \left(\sqrt{T_{B_k}} \frac{\mu_l}{\sigma_l}, \sqrt{x} \right) &= \frac{1}{\left(\sqrt{T_{B_k}} \frac{\mu_l}{\sigma_l} \right)^{\frac{T_{B_k}}{2}-1}} \int_{\sqrt{x}}^{\infty} x^{\frac{T_{B_k}}{2}} \cdot \\ &\exp \left(-\frac{x^2 + \left(\sqrt{T_{B_k}} \frac{\mu_l}{\sigma_l} \right)^2}{2} \right) \mathcal{I}_{\frac{T_{B_k}}{2}-1} \left(\sqrt{T_{B_k}} \frac{\mu_l}{\sigma_l} x \right) dx, \end{aligned} \quad (8)$$

is the Marcum Q-function [30] and $\mathcal{I}_\nu(\cdot)$ is the modified Bessel function of first kind of order ν [31].

E. Probability of Missed Detection

Missed detection occurs when $\|\mathbf{R}_{B_k}\|^2 = \sum_{j=1}^{T_{B_k}} y_j^2 \leq \gamma$, given that the user is present in the BG B_k . The probability of missed detection is evaluated as

$$\begin{aligned} p_m &= \mathbb{P} \left(\|\mathbf{R}_{B_k}\|^2 \leq \gamma \mid \mathbb{1}(B_k) = 1 \right) \\ &= \mathbb{P} \left(\frac{\|\mathbf{R}_{B_k}\|^2}{\sigma_1^2} \leq \frac{\gamma}{\sigma_1^2} \mid \mathbb{1}(B_k) = 1 \right) \\ &= 1 - \mathcal{Q}_{\frac{T_{B_k}}{2}} \left(\sqrt{T_{B_k}} \frac{\mu_1}{\sigma_1}, \frac{\sqrt{\gamma}}{\sigma_1} \right). \end{aligned} \quad (9)$$

Next, consider the arguments of the Marcum Q-function above as $a_1 = \sqrt{T_{B_k}} \frac{\mu_1}{\sigma_1}$ and $b_1 = \frac{\sqrt{\gamma}}{\sigma_1}$, respectively. Thus, we have

$$\begin{aligned} a_1^2 &= \frac{g' T_{B_k}}{N \sigma^2}, \\ b_1^2 &= \frac{\frac{4g g' \sigma^2}{2N g' - g} \left[1 - \sqrt{\frac{Ng}{2g'}} - T_{B_k} \left(\frac{g-G}{N \sigma^2} \right) \right]}{\frac{4\sigma^2 g'}{N}} \\ &= \frac{Ng}{\frac{2}{N} g' - g} \left[1 - \frac{Ng}{2g'} + T_{B_k} \frac{G-g}{\sigma^2 N} \right]. \end{aligned}$$

Corollary 1 (Chernoff-type bound). Clearly, $b_1^2 < \frac{T_{B_k}}{2} (a_1^2 + 2)$ and hence, for $0 < \lambda < \frac{1}{2}$ we can derive a Chernoff-type bound for the probability of missed detection as

$$p_m \leq (1 - 2\lambda)^{-\frac{T_{B_k}}{2}} \exp \left(-\lambda b_1^2 + \frac{\lambda T_{B_k} a_1^2}{2(1 - 2\lambda)} \right).$$

The detailed steps to derive the above bound can be found in [32] and is being skipped here for brevity. The optimal value for the Chernoff parameter λ is found by differentiation as

$$\lambda_1 = \frac{1}{2} \left(1 - \frac{T_{B_k}}{2b_1^2} - \frac{T_{B_k}}{2b_1^2} \sqrt{1 - \frac{2a_1^2 b_1^2}{T_{B_k}}} \right). \quad (10)$$

However, in such cases, p_m is trivially upper-bounded by 1. In order to derive a more meaningful bound, we note that

$$\lim_{g \rightarrow 0} a_1^2 = \frac{GT_{B_k}}{2\sigma^2 N}, \quad \lim_{g \rightarrow 0} b_1^2 = 0. \quad (11)$$

Following this observation, we derive the following bound on the probability of missed detection.

Lemma 2. For some $C_1 \geq 0$,

$$p_m \leq C_1 \exp \left(-\frac{GT}{2N\sigma^2 \log N} \right), \quad (12)$$

where $\lim_{g \rightarrow 0} C_1 = 0 \forall T$.

Proof: Please see Appendix A. ■

F. Probability of False Alarm

False alarm is raised when $\|\mathbf{R}_{B_k}\|^2 = \sum_{j=1}^{T_{B_k}} y_j^2 > \gamma$, given that the user is not present in the BG B_k . The probability of false alarm is evaluated as

$$\begin{aligned} p_f &= \mathbb{P} \left(\|\mathbf{R}_{B_k}\|^2 > \gamma \mid \mathbb{1}(B_k) = 0 \right) \\ &= \mathbb{P} \left(\frac{\|\mathbf{R}_{B_k}\|^2}{\sigma_0^2} > \frac{\gamma}{\sigma_0^2} \mid \mathbb{1}(B_k) = 0 \right) \\ &= \mathcal{Q}_{\frac{T_{B_k}}{2}} \left(\sqrt{T_{B_k}} \frac{\mu_0}{\sigma_0}, \frac{\sqrt{\gamma}}{\sigma_0} \right). \end{aligned} \quad (13)$$

Letting $a_0 = \sqrt{T_{B_k}} \frac{\mu_0}{\sigma_0}$ and $b_0 = \frac{\sqrt{\gamma}}{\sigma_0}$, respectively, we have

$$\begin{aligned} a_0^2 &= \frac{T_{B_k} g}{2\sigma^2}, \\ b_0^2 &= \frac{2g'}{\frac{2}{N} g' - g} \left[1 - \sqrt{\frac{Ng}{2g'}} + T_{B_k} \frac{(G-g)}{\sigma^2 N} \right]. \end{aligned}$$

Thus, we have

$$\lim_{g \rightarrow 0} b_0^2 = N + \frac{GT}{\sigma^2 N \log N}, \quad \lim_{g \rightarrow 0} a_0^2 = 0. \quad (14)$$

Following this observation, we derive the following bound on the probability of missed detection.

Lemma 3. For some $C_2 \geq 0$

$$p_f \leq C_2 \exp \left(-\frac{GT}{\sigma^2 N \log N} \right), \quad (15)$$

where $\lim_{g \rightarrow 0} C_0 = 0, \forall T$.

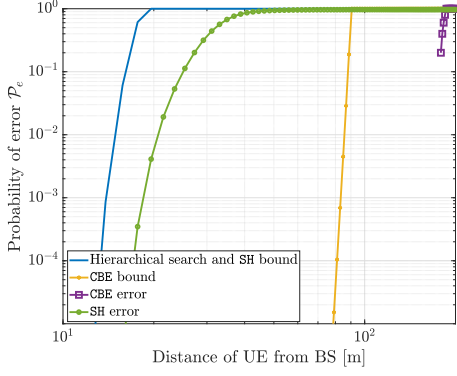


Fig. 2. Probability of beam selection error and error bounds with respect to the UE distance.

Proof: Please see Appendix B. ■

Interestingly, for p_f , the upper bound is tighter than the one for p_m due to the extra $\exp(-N)$ term in the former. Now we are in a position to state the main result for CBE.

Theorem 1. *With CBE, the probability of beam-selection error is upper bounded by*

$$\mathcal{P}_{\text{NC}}^{\text{CBE}}(T) \leq L_1 \log N \exp\left(-\frac{GT}{2N\sigma^2 \log N}\right),$$

where $L_1 = \max\{C_1, C_2\}$.

Proof: The proof follows from Lemma 2 and Lemma 3. Note that each beam \mathbf{f}_i belongs to v_i BGs, where $v_i = \{1, 2, \dots, \log N\}$. As an example, for $N = 16$, \mathbf{f}_1 belongs to only $\{B_1\}$ and hence, $v_1 = 1$ while \mathbf{f}_{15} belongs to $\{B_1, B_2, B_3, B_4\}$ and hence $v_{15} = 4$. The number of BGs a beam \mathbf{f}_i belongs to depends on the number of '1's in the binary representation of i . Accordingly, for the event that the user is present in beam \mathbf{f}_i for each i , the probability of beam selection error is upper bounded by

$$\begin{aligned} \mathcal{P}_{\text{NC}}^{\text{CBE}}(T) &\leq \nu_i p_m + (N - \nu_i) p_f \\ &\leq \log N \max\{p_m, p_f\} \\ &\leq \log N \max\{C_1, C_2\} \exp\left(-\frac{GT}{2N\sigma^2 \log N}\right). \end{aligned}$$

■

G. Comparison with Other Bounds

The bound derived in the work by Karnin *et al.* [33] for the probability of best arm selection error is $3 \log N \exp\left(-\frac{T}{8H_2 \log N}\right)$, where $H_2 := \max_{i \neq 1} \frac{i}{\Delta_i^2}$, which in our case is $\frac{N}{G-g}$ and hence the bound is $3 \log N \exp\left(-\frac{T(G-g)}{8N \log N}\right)$. We note that similar to hierarchical search, SH also discards half the possible beams for the codebook at each stage. Due to the result that $\lim_{g \rightarrow 0} L_1 = 0$, the bound derived by us for this case of thin and highly directional orthogonal beams is a much tighter one as compared to [33]. Of course, the additional assumption is that we allow for multi-beam concurrent transmission.

This is confirmed in Fig. 2 where we plot the bounds for the hierarchical search and for CBE with respect to the distance of

the UE from the BS. For comparison, we also plot the actual error evaluated using extensive Monte-Carlo simulations.

IV. BEST BEAM SELECTION IN AN ABRUPTLY CHANGING ENVIRONMENT

A. The SH Algorithm

The SH is a popular algorithm used for identifying the best arm in MAB problems. It evolves as a sequence of rounds. The total number of rounds is $\log N$. In our context, for each round, each beam is allocated an equal number of measurement time slots for transmission. Within each round, the reward of each beam is evaluated based on the allocated slots, i.e., the sum of the received power is measured. Then, the top half of beams (i.e., those with the highest observed rewards) are identified and the remaining beams are eliminated. Then, in the next round, the framework allocates an equal number of slots to each of the surviving beams. These steps are repeated until only one beam remains, which is considered the best beam based on the observed rewards. Thus, SH balances exploration and exploitation by gradually eliminating weaker beams and reallocating samples to the stronger beams. By allocating more measurement slots to beams with potentially higher rewards, it focuses exploration on the most promising options.

B. SH with a Single Abrupt Change

For this analysis, we make a minor change in the SH algorithm as compared to [33] - in each episode, instead of consecutive sampling from the same beam, we sample the beams in a round-robin manner. Naturally, this increases the possibility of sampling the beams post a change event. Let us consider the sample mean of the i -th beam at the end of the r -th round in case it does not experience a change -

$$\hat{\mu}_i(r) = \frac{1}{n_r} \sum_{t=1}^{n_r} R_i \left(\sum_{v=1}^{r-1} n_v + (i - |S_r|) + |S_r|t \right), \quad (16)$$

where $n_r = \frac{2^{r-1}T}{N \log N}$ is the number of times each beam is sampled in the round r . We simplify the time indices since the reward values for beam \mathbf{f}_i are i.i.d. as R_i in case of no changes. Thus the estimate of the mean of the beam \mathbf{f}_i at the end of episode r is given as

$$\hat{\mu}_i(r) = \frac{1}{n_r} \sum_{k=1}^{n_r} R_i(k) = \frac{1}{n_r} \|\mathbf{R}_i(r)\|^2.$$

Let the change occur in the reward distribution of the arm j in round r_c and consider that the reward values for arm j are i.i.d. as $R_j^- \sim \mathcal{N}(\mu_j^-, \sigma_j^-)$ before t_c and as $R_j^+ \sim \mathcal{N}(\mu_j^+, \sigma_j^+)$ after t_c . Consider the case that the change results in the arm j being the best arm for $t > t_c$, i.e., $\arg \max \mu_i(t) = j$ for $t > t_c$. If $j \in S_{r_c}$, its mean estimate is

$$\hat{\mu}_j(r_c) = \frac{1}{n_{r_c}} \left[\sum_{l=1}^{n'} R_j^-(l) + \sum_{m=1}^{n_{r_c}-n'} R_j^+(m) \right],$$

where n' is the slot in round r_c after which the change occurs. Let the conditional CDF that the change occurs in any slot n given r_c be given by $F_{n'}(n|n_{r_c})$.

C. Analysis for Round r_c

Recall that $S_{r_c} = \frac{N}{2^{r_c-1}}$ beams enter the round r_c and each beam is played $n_{r_c} = \frac{T}{|S_{r_c}| \log N}$ times. The probability, $p_{i,j}(r_c)$ that the arm j has a lower empirical mean than the arm $i \neq j$ after round r_c is calculated in the following lemma.

Lemma 4. *Given that the beams \mathbf{f}_i and \mathbf{f}_j survive until the round r_c in which \mathbf{f}_j undergoes a change, the probability that the estimate of the mean of \mathbf{f}_j is lower than that of \mathbf{f}_i after round r_c is*

$$p_{i,j}(r_c) \leq 1 - F_{n'}(n_i^* | n_{r_c}) \left(1 - \exp \left(-\frac{\Delta_{\min}^2 T}{2N \log N \sigma_{\max}^2} \right) \right), \quad (17)$$

where $n_i^* = -\frac{n_{r_c} \Delta_{i,j}^+}{\Delta_c}$ and $F_{n'}(\cdot | n_{r_c})$ is the conditional CDF of the change time slot given that the change occurs in the round r_c . Additionally, $\sigma_{\max}^2 = 2\sigma^2 \mu_{\max}$.

Proof: Please see Appendix C. ■

We note that the bound derived above has two parts - $1 - F_{n'}(n_i^* | n_{r_c})$ and $F_{n'}(n_i^* | n_{r_c}) \exp \left(-\frac{\Delta_{\min}^2 T}{2N \log N \sigma_{\max}^2} \right)$. Since we are interested in the event that \mathbf{f}_j survives the round, the sum of these terms needs to be less than or equal to 1 for the bound to be meaningful. Based on the difference of the means between the arms \mathbf{f}_i and \mathbf{f}_j before and after the change, the following four cases arise.

- 1) $\Delta_{i,j}^+ > 0$ and $\Delta_c > 0$, i.e., the beam \mathbf{f}_i is always superior to the beam \mathbf{f}_j . In this case, $p_{i,j}(r_c)$ is trivially upper bounded by 1.
- 2) $\Delta_{i,j}^+ < 0 < \Delta_c$ and $|\Delta_{i,j}^+| > |\Delta_c|$, i.e., the beam \mathbf{f}_i is always inferior to the beam \mathbf{f}_j . In this case, $F_{n'}(n_i^* | n_{r_c}) = 1$ and thus, $p_{i,j}(r_c)$ is exponentially bounded.
- 3) $\Delta_{i,j}^+ < 0 < \Delta_c$ and $|\Delta_{i,j}^+| < |\Delta_c|$, i.e., the beam \mathbf{f}_i is superior to \mathbf{f}_j before the change and it becomes inferior to the beam \mathbf{f}_j after the change. Here for a change at slot $n' \leq n_i^*$, $p_{i,j}(r_c)$ is exponentially bound, while for $n' > n_i^*$ it is trivially bounded by 1. Hence, in this case, the earlier the change, the higher the chance that \mathbf{f}_j survives with respect to \mathbf{f}_i .
- 4) $\Delta_c < 0 < \Delta_{i,j}^+$, i.e., \mathbf{f}_i is inferior to \mathbf{f}_j before the change and it becomes superior to \mathbf{f}_j after the change. Contrary to the previous case, here, for a change at slot $n' \leq n_i^*$, $p_{i,j}(r_c)$ is bounded by 1, while for $n' > n_i^*$ it is exponentially bounded. Hence, in this case, the later the change, the higher the chance that \mathbf{f}_j survives with respect to \mathbf{f}_i .

Out of the above, only cases 2 and 3 are of interest to us since we assume that after the change \mathbf{f}_j becomes the best beam. Let the change occur in the K -th best beam. Then, the following result bound its probability of elimination in the round r_c .

Lemma 5. *The probability that the K -th arm is eliminated in round r_c is upper bounded by*

$$p_K(r_c) \leq 2 \left[1 - F_{n'}(n_{\max}) \left(1 - \exp \left(-\frac{\Delta_{\min}^2}{2\sigma_{\max}^2} \right) \right) \right],$$

where $n_{\max} = \frac{n_{r_c} \Delta_{\min}}{\Delta_c}$.

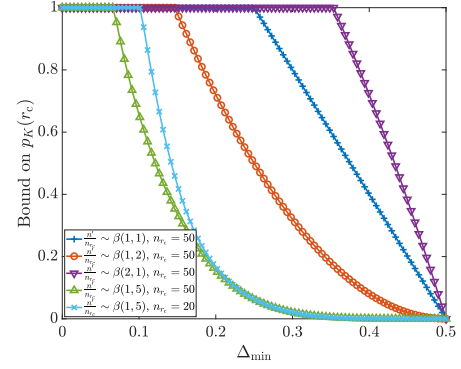


Fig. 3. Bound on $p_K(r_c)$ with respect to Δ_{\min} for different change distributions.

Proof: Let N_{r_c} denote the number of arms that have a higher estimated mean than the K -th arm in the round r_c . Then,

$$\begin{aligned} \mathbb{E}[N_{r_c}] &= \sum_{\mathbf{f}_i \in \mathcal{S}_{r_c}} \mathbb{P}(\hat{\mu}_i(r_c) > \hat{\mu}_K(r_c)) \\ &\leq \sum_{\mathbf{f}_i \in \mathcal{S}_{r_c}} 1 - F_{n'}(n_i^* | n_{r_c}) \left(1 - \exp \left(-\frac{\Delta_{\min}^2}{2\sigma_{\max}^2} \right) \right) \\ &\leq |\mathcal{S}_{r_c}| \left[1 - F_{n'}(n_{\max}) \left(1 - \exp \left(-\frac{\Delta_{\min}^2}{2\sigma_{\max}^2} \right) \right) \right]. \end{aligned} \quad (18)$$

Now, from Markov's inequality, we have

$$\mathbb{P} \left(N_{r_c} \geq \frac{|\mathcal{S}_{r_c}|}{2} \right) \leq \frac{2\mathbb{E}[N_{r_c}]}{|\mathcal{S}_{r_c}|}.$$

Substituting (18) in the above completes the proof. ■

Example 1. *In case the exact change slot is uniformly distributed in the round r_c , then we have $F_{n'}(n_{\max}) = \frac{n_{\max}}{n_{r_c}} = \frac{\Delta_{\min}}{\Delta_c}$. Accordingly, $p_K(r_c)$ is upper bounded as*

$$p_K(r_c) \leq 2 \left(1 - \frac{\Delta_{\min}}{\Delta_c} \left(1 - \exp \left(-\frac{\Delta_{\min}^2}{2\sigma_{\max}^2} \right) \right) \right). \quad (19)$$

For a given value of r_c (equivalently n_{r_c}) the exact location of the change is governed by its distribution. In this work we do not make any assumptions on the same, and hence, a beta distribution is appropriate to model its location [34]. First we note from Fig. 3 that higher the magnitude of change Δ_{\min} , the lower will be the bound on $p_K(r_c)$. More importantly, in case the changes occur earlier in the change round, i.e., the beta distribution is skewed to the left, the probability of elimination of \mathbf{f}_K is limited. In particular, we have the following important result.

Corollary 2. *For $r_c \leq r^*$,*

$$p_K(r_c) \leq 2K \exp \left(-\frac{\Delta_{\min}^2}{2\sigma_{\max}^2} \right). \quad (20)$$

Proof: This follows from Lemma 5 by recognizing that for all beams \mathbf{f}_i which are inferior to \mathbf{f}_K , we have $\Delta_{i,K}^+ < 0 < \Delta_c$ and $|\Delta_{i,K}^+| > |\Delta_c|$. Hence, $F_{n'}(n_i^*) = 1 \forall i > K$. Now, for \mathbf{f}_K to be eliminated, it has to be in the bottom half

of the estimated beams in the r_c -th round, at least $\frac{|\mathcal{S}_{r_c}|}{2} - K$ inferior beams should have a higher estimate than \mathbf{f}_K . Recall that the number of beams in the r_c -th round which are inferior to \mathbf{f}_K is $|\mathcal{S}_{r_c}| - K$. Hence,

$$\begin{aligned} \mathbb{P}\left(N_{r_c} \geq \frac{|\mathcal{S}_{r_c}|}{2} \mid r_c \leq r^*\right) &\leq \frac{|\mathcal{S}_{r_c}| - K}{\frac{|\mathcal{S}_{r_c}|}{2} - K} \exp\left(-\frac{\Delta_{\min}^2}{2\sigma_{\max}^2}\right) \\ &\leq 2K \exp\left(-\frac{\Delta_{\min}^2}{2\sigma_{\max}^2}\right). \end{aligned}$$

Next, we characterize the probability of eliminating the K -th arm ($1 \leq K \leq N$) in two distinct segments.

Early change - $r_c \leq r^*$

Lemma 6. *Conditioned on the change occurring within the first $r^* = \log \frac{N}{2K} + 1$ rounds, the probability that the best arm is eliminated is upper bounded as*

$$\mathcal{P}_C^{\text{SH}}(T \mid r_c \leq r^*) \leq 2(\log N + K - 1) \exp\left(-\frac{1}{2} \frac{\Delta_{\min}^2 T}{N \log N}\right).$$

Proof: Please see Appendix D. ■

Late change - $r_c > \log \frac{N}{2K}$

Lemma 7. *If the change after the first $\log \frac{N}{2K}$ rounds, the probability that the best arm is eliminated is upper bounded as*

$$\begin{aligned} \mathcal{P}_C^{\text{SH}}(T \mid r_c > r^*) &\leq \mathcal{T}_1(r_c) + \\ &2 \log 2NK \exp\left(-\frac{1}{2} \frac{\Delta_{\min}^2 T}{N \log N}\right). \end{aligned}$$

where $\mathcal{T}_1(r_c) = \mathbb{E}[r_c - r^* \mid r^* \leq r_c \leq \log N]$.

Proof: Please see Appendix E. ■

Thus, in case of late change, the bound has an exponential term and a term that depends on the distribution of the change slot location. Thus, in case of late change occurs in any round, SH does not achieve an exponential upper bound.

Theorem 2. *In case of a single abrupt change in the mean of \mathbf{f}_K at time $0 \leq t_c \leq T$, the bound on the beam selection error is given by*

$$\begin{aligned} \mathcal{P}_C^{\text{SH}} &= \mathcal{P}_C^{\text{SH}}(T \mid r_c \leq r^*) \mathbb{P}(r_c \leq r^*) + \\ &\mathcal{P}_C^{\text{SH}}(T \mid r_c > r^*) \mathbb{P}(r_c > r^*) \\ &\leq \mathcal{T}_1(r_c) + 2(2 \log N + K - 1) \exp\left(-\frac{1}{2} \frac{\Delta_{\min}^2 T}{N \log N}\right). \end{aligned}$$

Corollary 3. [No Change] *In case of no change, the performance of SH is exponentially bounded as $\log N \exp\left(-\frac{1}{2} \frac{\Delta_{\min}^2 T}{N \log N}\right)$ which is of the form given in [33].*

V. HYBRID POLICY FOR KNOWN K

Next, consider the case when the change is restricted to the top K beams of the system. This is typical for cases when the optimal beam is blocked initially. The beam-selection procedure recognizes an adjacent beam to the optimal beam as the best one for service initially. This is mainly due to

Algorithm 2 K-SHES

```

1: Input:  $[\mathbf{F}]$ .
2:  $\mathcal{S}_1 = [\mathbf{F}]$ .
3: Calculate  $r^* = \log \frac{N}{2K}$ .
4: for  $1 \leq r < r^*$  do
5:   Calculate  $n_r = \frac{T}{\log N 2^{r-1}}$ .
6:   for All  $\mathbf{f}_i \in \mathcal{S}_r$  do
7:     Measure received power  $R_i$  in slots  $k|\mathcal{S}_r + i|$  slots
       for  $k = 0, 1, \dots, n_r - 1$ .
8:     Evaluate  $\|\mathbf{R}_i\|^2$ .
9:   end for
10:  Rank the beams of  $\mathcal{S}_r$  in decreasing order of  $\|\mathbf{R}_i\|^2$ .
11:  Identify the set  $\mathcal{S}'_r$  bottom  $\frac{|\mathcal{S}_r|}{2}$  arms.
12:   $\mathcal{S}_{r+1} = \mathcal{S}_r \setminus \mathcal{S}'_r$ .
13: end for
14: From the remaining  $\mathcal{S}_{r^*+1}$  arms, identify the best beam
    using equal allocation.
15: Return: Optimal beam  $\mathbf{f}_j$ .

```

the correlation among the beams, directional transmissions, and limited multipath in mm-wave. However, in case the optimal beam abruptly transitions into a line-of-sight state during the beam-selection procedure, the algorithm must adapt and report only the optimal beam. In this regard, we propose K-SHES which exploits the knowledge of K to tune the SH appropriately. The steps of K-SHES is presented in Algorithm 2. For a given value of K , we calculate $r^* = \log \frac{N}{2K}$. Until the round r^* , K-SHES employs the classical SH algorithm, i.e., until the $2K$ arms are left. Once $2K$ beams are left, the algorithm does not further eliminate beams. After r^* , the remaining $\frac{N}{2^{r^*-1}}$ beams are sampled in a round-robin manner, and the best beam is determined at T based on received power in the slots after r^* .

Theorem 3. *The beam selection error for the K-SHES algorithm is given by*

$$\begin{aligned} \mathcal{P}_C^{\text{K-SHES}}(T) &\leq \mathcal{T}_{\text{K-SHES}} \exp\left(-\frac{1}{2} \frac{\Delta_{\min}^2 T}{2N \log N \sigma_{\max}^2}\right) + \\ &\sum_{i=1}^{K-1} 1 - F_{t_c}(t_i \mid r^*) \left(1 - \exp\left(-\frac{1}{2} \frac{\Delta_{\min}^2 T}{N \log N \sigma_{\max}^2}\right)\right). \end{aligned}$$

where $\mathcal{T}_{\text{K-SHES}} = \log \frac{N^2}{2K} + K(2 \log(2K) + 1)$. *If the change occurs in the first $T \left\lceil \frac{\log(N/2K)}{\log N} \left(1 - \frac{1}{2K}\right) + \frac{1}{2K} \right\rceil$ time slots with probability 1, then the beam selection error is exponentially bounded as*

$$\begin{aligned} \mathcal{P}_C^{\text{K-SHES}}(T) &\leq 2(2 \log N + 2K - 1) \cdot \\ &\exp\left(-\frac{1}{2} \frac{\Delta_{\min}^2 T}{2N \log N \sigma_{\max}^2}\right) \end{aligned} \quad (21)$$

Proof. Similar to the SH case, the upper bound on the error with K-SHES can be derived as a sum for the early and the late change cases. For both the early change and the late change cases, the analysis remains the same until the round r^* . Beyond r^* , due to a single round, the probability of beam-selection error is given by the union bound over the remaining

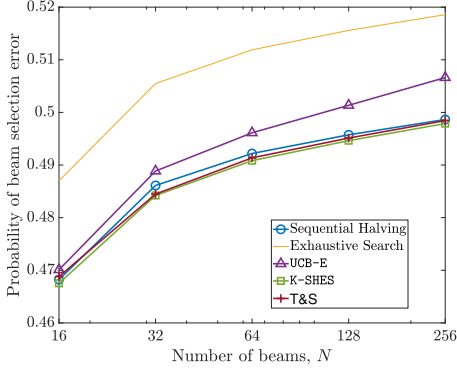


Fig. 4. Comparison in terms of beam selection error. Here $T = 1024 = 2^{10}$ and K belongs to the top 20 percent of the beams.

$2K$ arms similar to the exhaustive search case,

$$\mathbb{P}(\mathcal{E}_K([r^*, \log N]) \mid r_C \leq r^*) \leq 2K \exp\left(-\frac{1}{2} \frac{\Delta_{\min}^2}{N \log N \sigma_{\max}^2}\right)$$

While for the late change case, the analysis follows similarly to Lemma 5,

$$\mathbb{P}(\mathcal{E}_K([r^*, \log N]) \mid r_C > r^*) \leq \sum_{i=1}^{K-1} 1 - F_{t_c}(t_i \mid r^*) \left(1 - \exp\left(-\frac{1}{2} \frac{\Delta_{\min}^2}{N \log N \sigma_{\max}^2}\right)\right)$$

For the late change case, if the change occurs early enough so as to safeguard against the best arm prior to the change, K-SHES results in an exponential bound. \square

VI. NUMERICAL RESULTS AND DISCUSSION

A. Performance Comparison

Fig. 4 shows that K-SHES outperforms SH and the exhaustive search algorithms. However, due to the no elimination in the case of K-SHES, it suffers from a higher probability of error as compared to SH in case the changes occur early. In case of an early change, SH and K-SHES perform equally until r^* . However, beyond r^* , due to no further changes, SH performs better due to sequentially eliminating suboptimal beams. However, since K-SHES does not eliminate beams beyond r^* , it results in a higher beam selection error. This is elaborated in Fig. 5.

B. Communication-Sensing Trade-off

Next, let us study the efficacy of K-SHES from the perspective of a wireless communication system and the trade-offs arising from the same. Let the communication scheme be partitioned into beam refinement and downlink data transmission phases as shown in Fig. 6. The beam alignment phase of duration T is mapped to K-SHES developed in this paper. The data transmission phase is of duration T_D . In case of a larger N , each beam can be made highly directional which leads to a higher radiated power. However, a larger N results in a higher beam selection error and a reduced communication performance. In addition, for a fixed frame length T_{tot} , if a higher number of time slots is allotted to beam refinement,

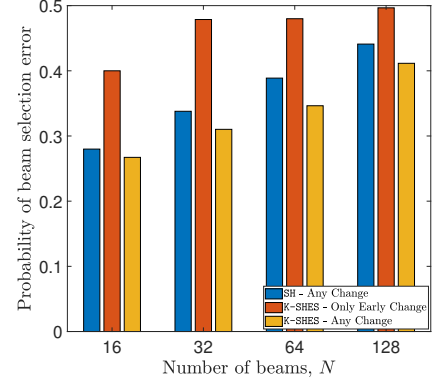


Fig. 5. Impact of the location of change. Here $T = 4096 = 2^{12}$ and K belongs to the top 20 percent of the beams.

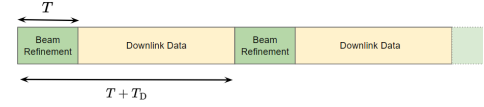


Fig. 6. Illustration of the communication scheme.

then fewer slots remain for data communication which may degrade the communication performance. On the contrary, fewer slots are reserved for beam refinement leads to a higher beam selection error and accordingly, a poor communication even with a large number of data transmission slots.

We assume that the user is stationary and is present at 100 m from the access point. The blockage condition can intermittently change uniformly within a frame. We assume a bandwidth of 1 GHz and a transmit power of 40 dBm. The impact of interference is ignored. The frame duration consists of 35072 slots. For a given number of beam N , we assume that the directivity gain per beam is $\frac{2\pi}{N}$ and accordingly, the downlink data rate is given by $(1 - \mathcal{P}_e) \frac{T_D}{T + T_D} W \log_2(1 + \xi_0)$, where ξ_0 is the reference signal to noise ratio (SNR) without the directivity gain. Here we have assumed that the side lobes have negligible power and hence, the received power in case of a beam misalignment is 0.

Fig. 7 shows that for a chosen T , there exists an optimal N . In case 1% of temporal resources allotted to beam alignment, the optimal beam number is 64, while for a higher number of resources allotted for beam alignment (10%), the optimal N

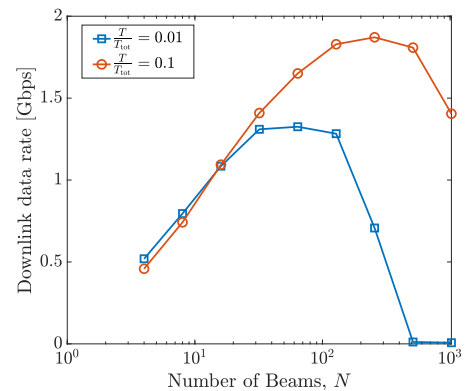


Fig. 7. Downlink data rate with respect to number of beams for different fraction of frames allotted to beam alignment.

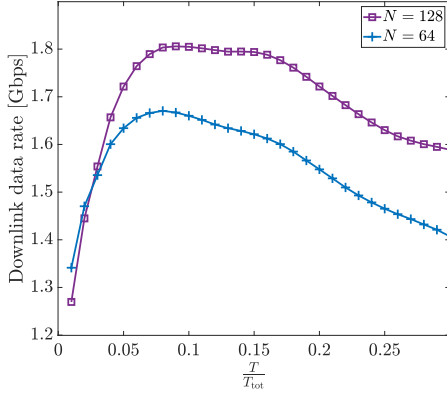


Fig. 8. Data rate with respect to the fraction of resources allotted to beam refinement phase for different sizes of beam dictionary.

increases to 128. Thus, for a larger beam alignment budget, a larger N can be employed to maximize the data rate. However, for low beam dictionary size, e.g., $N = 16$, $\frac{T}{T_{\text{tot}}} = 0.1$ is sufficient to achieve the best possible beam selection efficacy and increasing resources further for beam alignment simply reduces the data rate. Similarly, Fig. 8 shows that for a given N , there exists optimal partitioning of the temporal resources between beam alignment and data communication phases. For very stringent beam alignment deadline, e.g., $\frac{T}{T_{\text{tot}}} = 0.1$, a lower N is a better choice due to the low beam selection error. However, as the beam alignment budget increases, a higher N can be chosen for optimal data rate.

VII. CONCLUSION

For the stationary environment, our proposed beam selection scheme CBE outperforms the state of the art bandit algorithms in terms of the probability of error. For the non-stationary environment, we showed that the popular SH algorithm does not achieve an exponential error bound. For a know range of index of change, we proposed K-SHES that achieves an exponential bound and thus, can be employed in beam selection procedures where the state of the beams change during initial access. We employed K-SHES in a tandem beam refinement and data transmission scheme and highlighted key system design insights in terms of selection of beam codebook and partitioning of temporal resources. A detailed analysis of the type of *allowable* change distributions as well as handling multiple changes are indeed interesting directions of research and we are currently investigating the same. This will be reported in future work.

APPENDIX A PROOF OF LEMMA 2

Let $\zeta_1 = \frac{a_1}{b_1}$. Following (11) we have $\zeta_1 > 1$ for diminishing g and accordingly

$$p_m = 1 - \mathcal{Q}_{\frac{T_{B_k}}{2}}(a_1, b_1)$$

$$\stackrel{(a)}{\leq} \exp\left(-\frac{1}{2}(a_1^2 + b_1^2)\right) \sqrt{\mathcal{I}_0(2a_1b_1)} \sqrt{\frac{\zeta_1}{2(\zeta_1^2 - 1)}} \sqrt{\frac{2\left(1 - \frac{T_{B_k}}{2}\right)}{\zeta_1}}$$

$$\begin{aligned} &\stackrel{(b)}{\leq} \exp\left(-\frac{1}{2}(a_1^2 + b_1^2)\right) \exp(a_1b_1) \sqrt{\frac{\zeta_1}{2(\zeta_1^2 - 1)}} \sqrt{\frac{2\left(1 - \frac{T_{B_k}}{2}\right)}{\zeta_1}} \\ &\leq \exp\left(-\frac{a_1^2}{2}\right) \exp(a_1b_1) \sqrt{\frac{\zeta_1}{2(\zeta_1^2 - 1)}} \sqrt{\frac{2\left(1 - \frac{T_{B_k}}{2}\right)}{\zeta_1}} \\ &= C_1 \exp\left(-\frac{g'}{2\sigma^2} \frac{T}{N \log N}\right) \stackrel{(c)}{\leq} C_1 \exp\left(-\frac{GT}{2N\sigma^2 \log N}\right). \end{aligned}$$

$\mathcal{I}_0(\cdot)$ is the modified Bessel function of the first kind with order 0. Step (a) follows from the Cauchy-Schwarz inequality for the Marcum-Q function [35]. The step (b) follows from the following [36]

$$I_\nu(x) < \frac{\cosh x}{\Gamma(\nu+1) \left(\frac{x}{\nu}\right)^\nu} \leq \frac{x^\nu}{2^\nu \nu!} \exp(x) \implies \mathcal{I}_0(x) \leq \exp(x).$$

The step (c) follows from the definition of g' . Now consider

$$C_1 = \exp(a_1b_1) \sqrt{\frac{\zeta_1}{2(\zeta_1^2 - 1)}} \sqrt{\frac{2\left(1 - \frac{T_{B_k}}{2}\right)}{\zeta_1}}. \text{ Due to (11) we have } \lim_{g \rightarrow 0} \zeta_1 = \infty \text{ and thus, } \lim_{\zeta_1 \rightarrow \infty} \sqrt{\frac{\zeta_1}{2(\zeta_1^2 - 1)}} = 0, \quad \forall T, \text{ and } \lim_{g \rightarrow 0} \exp(a_1b_1) = 1. \text{ Thus, from the limit rule of product, we have } \lim_{g \rightarrow 0} C_1 = 0.$$

APPENDIX B PROOF OF LEMMA 3

The proof follows by considering $\zeta_0 = \frac{a_0}{b_0} < 1$ and applying the corresponding Cauchy-Schwarz bound for $\mathcal{Q}_{\frac{T_{B_k}}{2}}(a_0, b_0)$ -

$$p_f = \mathcal{Q}_{\frac{T_{B_k}}{2}}(a_0, b_0)$$

$$\begin{aligned} &\stackrel{(a)}{\leq} \exp\left(-\frac{1}{2}(a_0^2 + b_0^2)\right) \sqrt{\mathcal{I}_0(2a_0b_0)} \sqrt{\frac{\zeta_0}{2(\zeta_0^2 - 1)}} \sqrt{\frac{2\left(1 - \frac{T_{B_k}}{2}\right)}{\zeta_0}} \\ &\leq \exp\left(-\frac{1}{2}(a_0^2 + b_0^2)\right) \exp(a_0b_0) \sqrt{\frac{\zeta_0}{2(\zeta_0^2 - 1)}} \sqrt{\frac{2\left(1 - \frac{T_{B_k}}{2}\right)}{\zeta_0}} \\ &\leq \exp\left(-\frac{b_0^2}{2}\right) \exp(a_0b_0) \sqrt{\frac{\zeta_0}{2(\zeta_0^2 - 1)}} \sqrt{\frac{2\left(1 - \frac{T_{B_k}}{2}\right)}{\zeta_0}} \\ &= C_0 \exp\left(-\frac{GT}{2N\sigma^2 \log N}\right). \end{aligned}$$

Unlike p_m , the step (a) follows since $\zeta_0 < 0$. Now consider

$$C_0 = \exp(a_0b_0) \exp(-N) \sqrt{\frac{\zeta_0}{2(\zeta_0^2 - 1)}} \sqrt{\frac{2\left(1 - \frac{T_{B_k}}{2}\right)}{\zeta_0}}. \quad (22)$$

Due to (14) we have $\lim_{g \rightarrow 0} \zeta_0 = 0$ and accordingly,

$$\lim_{\zeta_0 \rightarrow 0} \sqrt{\frac{\zeta_0}{2(\zeta_0^2 - 1)}} = 0, \quad \forall T, \quad (23)$$

and $\lim_{g \rightarrow 0} \exp(a_0 b_0) = 1$. Thus, from the limit rule of product, we have $\lim_{g \rightarrow 0} C_1 = 0$.

APPENDIX C PROOF OF LEMMA 4

We have from the definition of $p_{i,j}(r_c)$,

$$\begin{aligned}
 p_{i,j}(r_c) &= \mathbb{P}(\hat{\mu}_i(r_c) - \hat{\mu}_j(r_c) > 0 \mid \mathbf{f}_i, \mathbf{f}_j \in S_{r_c}) \\
 &= \mathbb{P}\left(\frac{1}{n_{r_c}} \sum_{k=1}^{n_{r_c}} R_i(k) - \frac{1}{n_{r_c}} \left[\sum_{l=1}^{n'-1} R_j^-(l) + \sum_{m=1}^{n_{r_c}-n'+1} R_j^+(m) \right] > 0 \mid \mathbf{f}_i, \mathbf{f}_j \in S_{r_c}\right) \\
 &= \mathbb{P}\left(\frac{n'-1}{n_{r_c}} [\hat{\mu}_{i,n'-1} - \hat{\mu}_{j,n'-1}^-] + \frac{n_{r_c}-n'+1}{n_{r_c}} [\hat{\mu}_{i,n_{r_c}-n'+1} - \hat{\mu}_{j,n_{r_c}-n'+1}^+] > 0 \mid \mathbf{f}_i, \mathbf{f}_j \in S_{r_c}\right) \\
 &= \mathbb{P}\left([\hat{\mu}_{i,n_{r_c}} - \mu_i] + \frac{n'-1}{n_{r_c}} [\mu_j^- - \hat{\mu}_{j,n'-1}^-] + \frac{n_{r_c}-n'+1}{n_{r_c}} [\mu_j^+ - \hat{\mu}_{j,n_{r_c}-n'+1}^+] + \frac{n'-1}{n_{r_c}} \Delta_{i,j}^- + \frac{n_{r_c}-n'+1}{n_{r_c}} \Delta_{i,j}^+ > 0 \mid \mathbf{f}_i, \mathbf{f}_j \in S_{r_c}\right). \quad (24)
 \end{aligned}$$

Now, let us note that

$$\begin{aligned}
 Z &= [\hat{\mu}_{i,n_{r_c}} - \mu_i] + \frac{n'-1}{n_{r_c}} [\mu_j^- - \hat{\mu}_{j,n'-1}^-] + \\
 &\quad \frac{n_{r_c}-n'+1}{n_{r_c}} [\mu_j^+ - \hat{\mu}_{j,n_{r_c}-n'+1}^+] \sim \mathcal{N}(0, \sigma_{ij}'^2).
 \end{aligned}$$

Accordingly,

$$\begin{aligned}
 p_{i,j}(r_c) &\leq \frac{1}{\sum_{n'=0}^{n_{r_c}} q_n(n')} \sum_0^{n_i^*} \exp\left(-\frac{\Delta_{i,j}'^2}{2\sigma_{ij}'^2}\right) q_n(n') + \sum_{n_i^*}^{n_{r_c}} q_n(n') p_{e_3}(r_c) = \mathbb{P}(\mathcal{E}_K([r_c, \log N]) \mid \mathbb{1}(e_K(r^*)) = 0, r \leq r_c \leq r^*) \\
 &\leq \exp\left(-\frac{\Delta_{\min}^2}{2\sigma_{ij}'^2}\right) F_{n'}(n_i^*) + 1 - F_{n'}(n_i^*) \\
 &\leq \exp\left(-\frac{\Delta_{\min}^2 T}{4N \log N \sigma^2 \mu_{\max}}\right) F_{n'}(n_i^*) + 1 - F_{n'}(n_i^*).
 \end{aligned}$$

where in step (a), $\Delta_{i,j}' = \frac{n'-1}{n_{r_c}} \Delta_{i,j}^- + \frac{n_{r_c}-n'+1}{n_{r_c}} \Delta_{i,j}^+$, $\sigma_{ij}'^2 = \frac{\sigma_i^2}{n_{r_c}} + \frac{n' \sigma_j^{-2}}{n_{r_c}^2} + \frac{(n_{r_c}-n') \sigma_j^{+2}}{n_{r_c}^2}$.

APPENDIX D PROOF OF LEMMA 6

The analysis considers three phases - i) rounds before r_c , ii) the r_c -th round, and iii) the rounds after r_c .

For the rounds before r_c , let N_r' be the number of arms from the bottom $|S_r| - K$ arms that have the estimate of their means larger than the estimate of the K -th arm. We have $\forall r < r_c$

$$\mathbb{E}[N_r' \mid r < r_c \leq r^*] \leq \sum_{q=K+1}^{|S_r|} \exp\left(-\frac{1}{2} \Delta_{Kq}^2 n_r\right)$$

$$\leq (|S_r| - K - 1) \exp\left(-\frac{1}{2} \Delta_{\min}^2 \frac{T}{N \log N}\right).$$

Consequently, the probability that the K -th arm is eliminated in the r -th round ($r \leq r_c \leq r^*$) is upper bounded by

$$\begin{aligned}
 &\mathbb{P}\left(N_r' > \frac{|S_r|}{2} \mid r \leq r_c \leq r^*\right) \\
 &\leq \frac{2}{|S_r|} \left[(|S_r| - K - 1) \exp\left(-\frac{1}{2} \Delta_{\min}^2 \frac{T}{N \log N}\right) \right] \\
 &\leq 2 \exp\left(-\frac{1}{2} \Delta_{\min}^2 \frac{T}{N \log N}\right).
 \end{aligned}$$

Accordingly, the probability that the K -th arm is eliminated until the round r_c is upper bounded as

$$\begin{aligned}
 p_{e_1}(r_c) &= \mathbb{P}(\mathcal{E}_K([r_c-1]) \mid r_c \leq r^*) \\
 &\leq \mathbb{E}_{r_c \leq r^*} [r_c - 1] \left[2 \exp\left(-\frac{1}{2} \Delta_{\min}^2 \frac{T}{N \log N}\right) \right].
 \end{aligned}$$

Next, if the K -th arm survives until the r_c -th round, the probability that it is eliminated in the r_c -th round is evaluated as (following Lemma 5)

$$\begin{aligned}
 p_{e_2}(r_c) &= \mathbb{P}(\mathcal{E}_K(r) \mid \mathbb{1}(\mathcal{E}_K([r_c-1])) = 0, r \leq r_c \leq r^*) \\
 &\leq 2 \mathbb{E}_{r_c \leq r^*} [1 - F_{n'}(n_{\max}) (1 - \exp\left(-\frac{T \Delta_{\min}^2}{2N \log N \sigma_{\max}^2}\right))] \\
 &\stackrel{(a)}{\leq} K \exp\left(-\frac{T \Delta_{\min}^2}{2N \log N \sigma_{\max}^2}\right).
 \end{aligned}$$

Step (a) is because before r^* only 1 arm among the set of beams inferior to the K -th beams needs a higher estimate than the K -th arm for it to be eliminated. Finally, given that the K -th arm has survived until the end of r_c the probability it is eliminated at the end of the play is upper bounded as

Thus, the total probability that the arm K is eliminated given that the change occurs in the first $\log \frac{N}{2K}$ rounds is upper bounded using the union bound as

$$\begin{aligned}
 &\mathbb{P}(\mathcal{E}_K([\log N]) \mid r_c \leq r^*) \\
 &\leq \mathbb{E}[p_{e_1}(r_c) + p_{e_2}(r_c) + p_{e_3}(r_c) \mid r_c \leq r^*] \\
 &\leq \mathbb{E}_{r_c, n'} \left[(r_c - 1) \left[2 \exp\left(-\frac{1}{2} \frac{\Delta_{\min}^2 T}{N \log N}\right) \right] + \left[K \exp\left(-\frac{1}{2 \sigma_{\max}^2} \frac{\Delta_{\min}^2 T}{N \log N}\right) \right] + 2(\log N - r_c) \left[\exp\left(-\frac{1}{2} \frac{\Delta_{\min}^2 T}{N \log N}\right) \right] \mid r_c \leq r^* \right].
 \end{aligned}$$

APPENDIX E PROOF OF LEMMA 7

We have $\forall r < r^*$

$$\mathbb{E}[N_r' \mid r \leq r^* \leq r_c] \leq \sum_{q=K+1}^{|S_r|} \exp\left(-\frac{1}{2} \Delta_{Kq}^2 n_r\right)$$

$$\leq (|\mathcal{S}_r| - K - 1) \exp\left(-\frac{1}{2}\Delta_{\min}^2 \frac{T}{N \log N}\right).$$

Consequently, the probability that the K -th arm is eliminated in the r -th round ($r \leq r^* \leq r_c$) is upper bounded by

$$\begin{aligned} & \mathbb{P}\left(N'_r > \frac{|\mathcal{S}_r|}{2} \mid r \leq r_c \leq r^*\right) \\ & \leq \frac{2}{|\mathcal{S}_r|} \left[(|\mathcal{S}_r| - K - 1) \exp\left(-\frac{1}{2}\Delta_{\min}^2 \frac{T}{N \log N}\right) \right] \\ & \leq 2 \exp\left(-\frac{1}{2}\Delta_{\min}^2 \frac{T}{N \log N}\right). \end{aligned}$$

Accordingly, the probability that the K -th arm is eliminated until the round r_* is upper bounded as

$$\begin{aligned} p_{l_1}(r_c) &= \mathbb{P}(\mathcal{E}_K([r^*]) \mid r_c > r^*) \\ &\leq 2r^* \exp\left(-\frac{1}{2}\Delta_{\min}^2 \frac{T}{N \log N}\right). \end{aligned}$$

Given that the K -th arm has survived until the end of r_{c_2} the probability it is eliminated at the end of the play is upper bounded as

$$p_{l_2}(r_{c_2}) = 2(\log N - r_c) \exp\left(-\frac{1}{2}\Delta_{\min}^2 \frac{T}{N \log N}\right). \quad (25)$$

Thus, the total probability that the arm K is eliminated given that the change occurs in the first $\log \frac{N}{2K}$ rounds is given by

$$p_l \leq \mathcal{T}_2(r_c) + 2 \log N \exp\left(-\frac{1}{2}\Delta_{\min}^2 \frac{T}{N \log N}\right). \quad (26)$$

REFERENCES

- [1] Y. Niu *et al.*, “A survey of millimeter wave communications (mmWave) for 5G: opportunities and challenges,” *Wireless networks*, vol. 21, pp. 2657–2676, 2015.
- [2] —, “Blockage robust and efficient scheduling for directional mmWave WPANs,” *IEEE Transactions on Vehicular Technology*, vol. 64, no. 2, pp. 728–742, 2014.
- [3] Z. Marzi *et al.*, “Compressive channel estimation and tracking for large arrays in mm-wave picocells,” *IEEE Journal of Selected Topics in Signal Processing*, vol. 10, no. 3, pp. 514–527, 2016.
- [4] M. Giordani *et al.*, “Initial access in 5G mmWave cellular networks,” *IEEE communications Magazine*, vol. 54, no. 11, pp. 40–47, 2016.
- [5] T. S. Cousik *et al.*, “Fast initial access with deep learning for beam prediction in 5G mmWave networks,” in *MILCOM 2021-2021 IEEE Military Communications Conference (MILCOM)*. IEEE, 2021, pp. 664–669.
- [6] G. Ghatak *et al.*, “Beamwidth optimization and resource partitioning scheme for localization assisted mm-wave communication,” *IEEE Transactions on Communications*, vol. 69, no. 2, pp. 1358–1374, 2020.
- [7] Z. Lin *et al.*, “SS/PBCH block design in 5G new radio (NR),” in *2018 IEEE Globecom Workshops (GC Wkshps)*. IEEE, 2018, pp. 1–6.
- [8] I. Aykin *et al.*, “Multi-beam transmissions for blockage resilience and reliability in millimeter-wave systems,” *IEEE Journal on Selected Areas in Communications*, vol. 37, no. 12, pp. 2772–2785, 2019.
- [9] J. Wang *et al.*, “Beam codebook based beamforming protocol for multi-Gbps millimeter-wave WPAN systems,” *IEEE Journal on Selected Areas in Communications*, vol. 27, no. 8, pp. 1390–1399, 2009.
- [10] J. Sung *et al.*, “Compressed-sensing based beam detection in 5G NR initial access,” in *2020 IEEE 21st International Workshop on Signal Processing Advances in Wireless Communications (SPAWC)*. IEEE, 2020, pp. 1–5.
- [11] H. Soleimani *et al.*, “Fast initial access for mmWave 5G systems with hybrid beamforming using online statistics learning,” *IEEE Communications Magazine*, vol. 57, no. 9, pp. 132–137, 2019.
- [12] T. S. Cousik *et al.*, “Deep Learning for Fast and Reliable Initial Access in AI-Driven 6G mm Wave Networks,” *IEEE Transactions on Network Science and Engineering*, 2022.
- [13] F. Sahrabi *et al.*, “Deep active learning approach to adaptive beamforming for mmWave initial alignment,” *IEEE Journal on Selected Areas in Communications*, vol. 39, no. 8, pp. 2347–2360, 2021.
- [14] F. Jiang *et al.*, “High-dimensional channel estimation for simultaneous localization and communications,” in *2021 IEEE Wireless Communications and Networking Conference (WCNC)*. IEEE, 2021, pp. 1–6.
- [15] S. Weng *et al.*, “Wideband mmWave Massive MIMO Channel Estimation and Localization,” *IEEE Wireless Communications Letters*, 2023.
- [16] H. Echigo *et al.*, “A deep learning-based low overhead beam selection in mmWave communications,” *IEEE Transactions on Vehicular Technology*, vol. 70, no. 1, pp. 682–691, 2021.
- [17] Y. Yang *et al.*, “Machine learning enabling analog beam selection for concurrent transmissions in millimeter-wave V2V communications,” *IEEE Transactions on Vehicular Technology*, vol. 69, no. 8, pp. 9185–9189, 2020.
- [18] S. Foo, “Orthogonal-Beam-Space Massive-MIMO Array,” in *2015 IEEE-APS Topical Conference on Antennas and Propagation in Wireless Communications (APWC)*. IEEE, 2015, pp. 320–324.
- [19] A. Alkhateeb *et al.*, “Initial Beam Association in Millimeter Wave Cellular Systems: Analysis and Design Insights,” *IEEE Transactions on Wireless Communications*, vol. 16, no. 5, pp. 2807–2821, 2017.
- [20] W. Wu *et al.*, “Fast mmwave beam alignment via correlated bandit learning,” *IEEE Transactions on Wireless Communications*, vol. 18, no. 12, pp. 5894–5908, 2019.
- [21] M. Hashemi *et al.*, “Efficient beam alignment in millimeter wave systems using contextual bandits,” in *IEEE INFOCOM 2018-IEEE Conference on Computer Communications*. IEEE, 2018, pp. 2393–2401.
- [22] V. Va *et al.*, “Online learning for position-aided millimeter wave beam training,” *IEEE Access*, vol. 7, pp. 30 507–30 526, 2019.
- [23] M. Hussain *et al.*, “Second-best beam-alignment via bayesian multi-armed bandits,” in *2019 IEEE Global Communications Conference (GLOBECOM)*. IEEE, 2019, pp. 1–6.
- [24] Y. Wei *et al.*, “Fast Beam Alignment via Pure Exploration in Multi-Armed Bandits,” *IEEE Transactions on Wireless Communications*, vol. 22, no. 5, pp. 3264–3279, 2023.
- [25] Y. Li *et al.*, “Design and analysis of initial access in millimeter wave cellular networks,” *IEEE Transactions on Wireless Communications*, vol. 16, no. 10, pp. 6409–6425, 2017.
- [26] I. Aykin *et al.*, “Efficient Beam Sweeping Algorithms and Initial Access Protocols for Millimeter-Wave Networks,” *IEEE Transactions on Wireless Communications*, vol. 19, no. 4, pp. 2504–2514, 2020.
- [27] M. Hellman *et al.*, “Probability of error, equivocation, and the Chernoff bound,” *IEEE Transactions on Information Theory*, vol. 16, no. 4, pp. 368–372, 1970.
- [28] R. W. Hamming, “Error Detecting and Error Correcting Codes,” *The Bell system technical journal*, vol. 29, no. 2, pp. 147–160, 1950.
- [29] G. Ghatak, “Actively tracking the best arm in non-stationary environments with mandatory probing,” *21st International Symposium on Modeling and Optimization in Mobile, Ad hoc, and Wireless Networks (WiOpt), Singapore 2023. Extended version at arXiv:2205.10366 [cs.LG]*, 2023.
- [30] D. A. Shnidman, “The calculation of the probability of detection and the generalized Marcum Q-function,” *IEEE Transactions on Information Theory*, vol. 35, no. 2, pp. 389–400, 1989.
- [31] F. Bowman, *Introduction to Bessel functions*. Courier Corporation, 2012.
- [32] Simon, M.K. and Alouini, M.-S., “Exponential-type bounds on the generalized marcum q-function with application to error probability analysis over fading channels,” *IEEE Transactions on Communications*, vol. 48, no. 3, pp. 359–366, 2000.
- [33] Z. Karnin *et al.*, “Almost optimal exploration in multi-armed bandits,” in *International Conference on Machine Learning*. PMLR, 2013, pp. 1238–1246.
- [34] A. K. Gupta *et al.*, *Handbook of beta distribution and its applications*. CRC press, 2004.
- [35] A. Annamalai *et al.*, “Cauchy-Schwarz bound on the generalized Marcum Q-function with applications,” *Wireless Communications and Mobile Computing*, vol. 1, no. 2, pp. 243–253, 2001.
- [36] Y. L. Luke, “Inequalities for generalized hypergeometric functions,” *Journal of Approximation Theory*, vol. 5, no. 1, pp. 41–65, 1972.